

Seasonal groundwater turnover

Maria Engström and Bo Nordell*

Division of Renewable Energy, Luleå University of Technology, SE-971 87 Luleå, Sweden.

*Corresponding author. E-mail: bon@ltu.se

Received 7 July 2004; accepted in revised form 16 September 2005

Abstract Seasonal air temperature variations and corresponding changes in groundwater temperature cause convective movements in groundwater similar to the seasonal turnover in lakes. Numerical simulations were performed to investigate the natural conditions for thermally driven groundwater convection to take place. Thermally driven convection could be triggered by a horizontal groundwater flow. Convection then starts at a considerably lower Rayleigh number (Ra) than the general critical Rayleigh number (Ra_c) assuming that 10°C groundwater is cooled to 4°C, i.e. heated from below convection in porous media. This study supports the hypothesis that seasonal temperature variations, under certain conditions, initiate and drive thermal convection.

Keywords Groundwater; seasonal turnover; simulation; temperature variation; thermal convection

Nomenclature

c_p	heat capacity	$\text{J kg}^{-1} \text{K}^{-1}$
D_p	grain size	mm
g	gravitational acceleration	m s^{-2}
H	depth of control volume	m
k	thermal conductivity	$\text{W m}^{-1} \text{K}^{-1}$
K	permeability	m^2
L	length of control volume	m
P	pressure	Pa
Q	heat transfer rate	W m^{-2}
Ra	Rayleigh number	
Ra_c	critical Rayleigh number	
T	time	s
T	temperature	°C
T_0	temperature of max. density	°C
T_H	bottom (hot) temperature	°C
T_C	top (cold) temperature	°C
u	horizontal Darcy velocity	m s^{-1}
v	vertical Darcy velocity	m s^{-1}
V_i	initial velocity	m s^{-1}
x	Cartesian coordinate	
y	Cartesian coordinate	

Greek symbols

α	thermal diffusivity	$\text{m}^2 \text{s}^{-1}$
γ	coefficient	$^{\circ}\text{C}^{-2}$

μ	dynamic viscosity	$\text{kg m}^{-1} \text{s}^{-1}$
ρ	density	kg m^{-3}
π	constant pi	
ρ_0	density maximum	kg m^{-3}
σ	heat capacity ratio	
ν	kinematic viscosity	$\text{m}^2 \text{s}^{-1}$
ϕ	porosity	%

Other symbols

$()_f$	fluid related
$()_s$	solid related

Introduction

Nutrient loss to groundwater leads to overfeeding of lakes and watercourses, negatively impacting flora and fauna. By understanding the mechanisms behind the leakage, fertilising could be done more effectively. Such knowledge would also be helpful in preventing and counteracting other types of contamination by leakage from ground surface to groundwater (Kyllmar and Johnsson 1998).

Seasonal turnover in lakes is well understood (SNA 1995). A thermal stratification of lake water forms due to a stable density distribution, with the densest water at the bottom of the lake. Because the uppermost layer of water is heated or cooled, this stratification is dissolved by the resulting density changes during spring and autumn. The temperature of the whole lake is temporarily equal before the temperature distribution is “turned upside down”. The driving force of thermal convection is the seasonal temperature variation of the surface water and its temperature-dependent density and viscosity. This mechanism is here applied as a “heated from below seasonal groundwater turnover”. The penetration depth depends on the size of the thermal gradient and hydraulic conductivity of the soil.

Our hypothesis is that the seasonal temperature variation initiates and drives thermal groundwater convection (Figure 1). The development is different in northern and southern Sweden, due to their different mean groundwater temperatures.

The maximum density temperature of water is close to 4°C. In southern Sweden with a mean groundwater temperature of 10°C the uppermost layer of the groundwater is cooled to 4°C in the autumn. This dense water begins to sink while the warmer less dense water below starts to rise and a convection roll is being formed. In northern Sweden with a mean groundwater temperature below 4°C the density increase takes place in the spring when the uppermost groundwater layer is heated to 4°C. If there is a melting frost layer the mean groundwater temperature is constantly 0°C.

During the autumn cold air causes a heat transport (radiative and convective) from ground surface to air that lowers the ground surface temperature. This induces a conductive heat

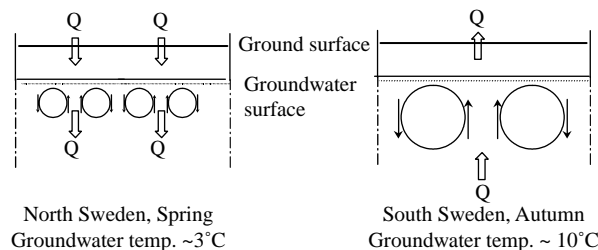


Figure 1 Outline of how heating or cooling drives groundwater convection. Groundwater mixing reaches greater depths in the south of Sweden since the groundwater mean temperature deviates more from the maximum density water temperature (4°C)

transport from the groundwater to the ground surface which lowers the temperature of the uppermost groundwater. Conductive heat transport through the soil cover depends on the soil depth (groundwater depth), soil thermal conductivity and the temperature difference between groundwater and ground surface (Claesson *et al.* 1985a).

Natural convection in fluid-saturated porous media is well covered in the heat transfer literature because of its many engineering applications (Nield and Bejan 1999). Performed studies in saturated porous media with nonlinear density distribution usually consider convection in thin layers, up to a few centimetres. Our problem involves convection rolls up to a few metres. Convection in aquifers has been studied at much higher temperatures in geological formations (Pestov 2000) and in thermal energy storage in aquifers (Claesson *et al.* 1985b).

Scope

A new approach to understand the mechanism of leakage from agricultural land as a result of thermally driven groundwater convection is suggested. This approach is numerically studied here and at this stage only groundwater movement is considered. Some assumptions were made on natural conditions and also prerequisites for the simulation model.

A constant groundwater table close to the ground surface and no horizontal groundwater flow was assumed. The permeability and the thermal conductivity are constant in the vertical and horizontal directions. It was also assumed that the driving energy of the convection is the heat transport from the warmer ground up to the ground surface. Melt water and rain infiltration that also influence the temperature gradient are not considered in this study.

At the upper and lower boundary of the simulated groundwater volume the temperatures are held constant. An initial disturbance is necessary to start the convection and an initial horizontal velocity was therefore introduced. Other natural disturbances, like inclined groundwater surface, heterogeneous permeability and varying thermal conductivity of the soil, were not considered.

Theory of thermal convection

By changing a fluid's temperature, a density and viscosity change occurs that stimulates the motion of a fluid (Rehbinder *et al.* 1995). This also happens when the fluid fills up a permeable material, e.g. groundwater in soil, even though the porous material slows down the velocity of the water. It is assumed that the fluid's temperature is equal to the matrix's temperature. Heat is transported by convection and conduction in the fluid and by conduction only in the matrix (Ene and Polisevski 1987).

Blake *et al.* (1984) provide the mathematical formulation of the thermal convection in porous media near 4°C. The conservation of mass, momentum and energy for the homogenous porous medium model are

$$\frac{\partial u}{\partial x} + \frac{\partial v}{\partial y} = 0 \quad (1)$$

$$u = -\frac{K}{\mu} \frac{\partial P}{\partial x} \quad (2)$$

$$v = -\frac{K}{\mu} \left(\frac{\partial P}{\partial y} + \rho g \right) \quad (3)$$

$$\sigma \frac{\partial T}{\partial t} + u \frac{\partial T}{\partial x} + v \frac{\partial T}{\partial y} = \alpha \left(\frac{\partial^2 T}{\partial x^2} + \frac{\partial^2 T}{\partial y^2} \right) \quad (4)$$

where the variables u and v are the fluid velocity components, P is pressure, ρ is density, t is time, and T is temperature. The constant K is the (intrinsic) permeability of the porous

matrix, μ is the viscosity, α is the thermal diffusivity, and g is the gravitational acceleration. The heat capacity ratio σ is defined as

$$\sigma = \frac{\varphi(\rho c_p)_f + (1 - \varphi)(\rho c_p)_s}{(\rho c_p)_f} \quad (5)$$

where φ is the porosity of the medium and $(\rho c_p)_f$ and $(\rho c_p)_s$ are the heat capacity of the fluid and solid matrix respectively. The usual Boussinesq approximation of temperature-dependent density cannot be used in this case. The density function of temperature is not linear close to the density maximum of $T_0 = 3.98^\circ\text{C}$. Therefore, a better, nonlinear approximation is that of [Goren \(1966\)](#) and [Moore and Weiss \(1973\)](#):

$$\rho = \rho_0(1 - \gamma(T - T_0)^2) \quad (6)$$

where ρ_0 is the maximum density of the water at T_0 and $\rho = 8 \times 10^{-6} (\text{C}^{-2})$. Equation (6) is valid in the temperature range of $0\text{--}10^\circ\text{C}$. Eliminating pressure from Equations (3) and (4) and incorporating Equation (6) leads to the single momentum conservation statement

$$\frac{\partial u}{\partial y} - \frac{\partial v}{\partial x} = -2 \frac{K \gamma g}{v} (T - T_0) \frac{\partial T}{\partial x} \quad (7)$$

Here the kinematic viscosity v is taken as μ/ρ_0 . The dynamic viscosity of a fluid, μ , is a second-order function of temperature between $0\text{--}10^\circ\text{C}$. The viscosity function used is derived from tabled values ([Fysikalia 1991](#)):

$$\mu = 0.11 \times 10^{-3} - 0.74 \times 10^{-6} T + 0.12 \times 10^{-8} T^2 \quad (8)$$

The Rayleigh number (Ra) is the balance between buoyant and viscous force, ([Kundu 1990](#)). In porous media Ra can be derived from the system of Equations (1)–(7), when Equation (7) is written in non-dimensional form. Ra is a non-dimensional constant and an eigenvector in the solution of the non-dimensional systems of equations ([Nield and Bejan 1999](#)). Ra can be written as

$$Ra = \frac{g K \gamma (T - T_0)^2 H}{\alpha v} \quad (9)$$

where H is the depth of the control volume. The general critical Rayleigh number, $Ra_c = 4\pi^2$ indicates that convection occurs for $Ra > Ra_c$.

Thermally driven convection could, however, be triggered and partly driven by a horizontal groundwater flow. Convection then starts at a lower Ra number. This phenomenon has been the subject of detailed studies in the field of aquifer thermal energy storage ([Claesson et al. 1985b](#)). [Nield and Bejan \(1999\)](#) analysed Ra for different boundary conditions and showed that it was possible to get lower critical Ra numbers than the general $Ra_c = 4\pi^2$ by introducing an initial horizontal groundwater movement (disturbance).

The Nusselt (Nu) number is defined as the ratio between actual heat transfer and conductive heat transfer. With a given geometry we get

$$Nu = \frac{Q}{kL(T_H - T_C)/H} \quad (10)$$

where k is the thermal conductivity of the water saturated porous matrix and Q is the overall heat transfer rate. Thus, convective heat transfer entails $Nu > 1$. In the performed calculations the converging Nu was used as a criterion for the stability of the numerical simulations.

Simulations

The simulation model FLUENT and the Finite Volume Method (FVM) were used to simulate the occurrence of the convection rolls (Versteeg and Malalasekera 1995).

A suitable mesh size for the simulations was first determined. Steady-state calculations were then performed to analyse how permeability and leakage depth influenced the formation of convection rolls.

Additionally, the effect of horizontal groundwater flow on thermal convection was evaluated. Here transient simulations gave the time for steady-state convection pattern to establish.

Calculation parameters

A 2D control volume is filled by a porous material and water where H (m) is the depth of the control volume and L (m) is the length of the same, see Figure 2. Heat is transported across the upper and lower boundaries. The permeability is assumed equal in both vertical and horizontal directions and the local temperature T is equal in both porous material and water. The constant boundary temperatures are $T_C = 4^\circ\text{C}$ and $T_H = 10^\circ\text{C}$ at the top and bottom of the control volume, respectively. There is no groundwater flow through the control volume, but an initial horizontal velocity V_i (m/s) is needed to start the convection. This is required by the simulation model but does not affect calculated convection velocities. A grid of quadratic mesh cells was used over the control volume.

Typical porosity values in sand are 35–50% for grain sizes of the order of 0.5–2.0 mm. To simplify the simulations, the porous material is assumed to consist of spherical grains of equal size, i.e. that the porosity is kept constant at 35%. By varying the grain size, Ra differs because of the permeability change. The (intrinsic) permeability, K (m^2), as given by Nield and Bejan (1999), is

$$K = \frac{D_p^2 \phi^3}{180(1 - \phi)^2} \quad (11)$$

where D_p is the grain size and ϕ is the porosity.

Results

Stable thermal convection occurs when $Nu > 1$ and $Ra > Ra_c$. In reality this means that thermal convection is influenced by soil permeability, thermal properties of the soil, temperature difference and distance (H) between the uppermost and undisturbed groundwater. The results are summarized in Table 1, where the permeability is a function of grain size. Formed rolls indicate stable convection within the control volume. In some cases no stable solution was found though $Nu > 1$, which means that part of the heat transport must be a result of convective heat transfer.

The numerical modelling requires that the analysed groundwater volume is big enough (L , H) for convection to take place. It also requires that the mesh size is small enough to

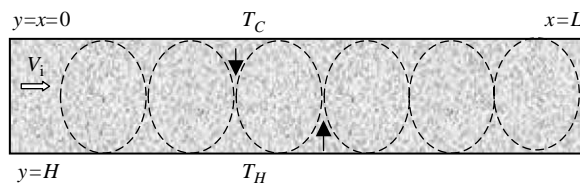


Figure 2 Vertical section of a control volume with the length L and depth H . The upper boundary is at constant temperature T_C and the lower boundary is at constant temperature T_H , where $T_H > T_C$. V_i is the initial velocity and the rolls represent the expected pattern

Table 1 Numerical results of how convection is influenced by mesh size, permeability (grain size) and depth

L (m)	H (m)	Mesh size (m)	$K (\times 10^{-9})$ (m^2)	Grain size (mm)	Ra (-)	Nu (-)	Roll size (m)	No. rolls (-)
Part 1								
10	1	0.150	0.67	1	19	1.97	0.83	12
10	1	0.100	0.67	1	19	2.05	0.83	12
10	1	0.050	0.67	1	19	2.14	0.83	12
10	1	0.025	0.67	1	19	2.14	0.83	12
Part 2								
10	1	0.05	2.71	2.00	76	5.2	0.38	26
10	1	0.05	2.07	1.75	59	4.42	0.45	22
10	1	0.05	1.52	1.50	43	3.61	0.56	18
10	1	0.05	1.06	1.25	30	2.92	0.63	16
10	1	0.05	0.67	1.00	19	2.14	0.83	12
10	1	0.05	0.38	0.75	11	1.16	-	-
10	1	0.05	0.17	0.50	5	1.16	-	-
Part 3								
10	1	0.05	0.67	1	19	2.14	0.83	12
10	2	0.10	0.67	1	38	1.66	1.25	8
10	3	0.10	0.67	1	57	1.42	1.25	8
10	4	0.10	0.67	1	76	-	-	-
10	5	0.10	0.67	1	95	1.17	2.5	4
10	6	0.10	0.67	1	114	1.11	2.5	4
10	7	0.10	0.67	1	134	-	-	-
10	8	0.10	0.67	1	153	-	-	-

analyse the groundwater movement. The mesh size of a fixed control volume (10×1 m) was therefore systematically reduced from 0.15 m to 0.025 m, see [Table 1](#) (Part 1). It is seen that Nu converges (at 2.14) with decreasing cell size which thus gives the maximum cell size to 0.05 m. Subsequently at least 20 mesh cells in the vertical direction were used to achieve converged solutions in the different control volumes. [Figure 3](#) pictures the stream function, temperature distribution and Nu for part of the 10×1 m control volume under assumed standard conditions.

The permeability was varied from 0.17 to $2.71 \times 10^{-9} m^2$, corresponding to grain sizes from 0.5–2 mm, in a fixed control volume. [Table 1](#) (Part 2) shows stable convection for $Ra > 19$ which equals a grain size of 1 mm, i.e. well below the general Ra_c . [Nield and Bejan \(1999\)](#) also observed similar results.

[Table 1](#) (Part 3) shows the influence of varying depth (H) for $K = 6.7 \times 10^{-10} m^2$ (grain size 1 mm), i.e. the lowest permeability for which stable convection occurred in Part 1. Stable convection exists for depths down to 6 m with a decreasing number of rolls. In the 4 m case no convection exists because the expected 6 rolls do not fit within the chosen control volume. [Figure 4](#) shows the result of a simulation of a 10×5 m control volume. Four convection rolls appear in symmetrical pattern acting in pairs (left). The corresponding groundwater temperature is also seen (right).

In previous simulations no horizontal groundwater flow was assumed. To investigate the importance of horizontal groundwater flow on thermal convection, flow velocities of $3 \times 10^{-9} m/s$, $3 \times 10^{-7} m/s$ and $3 \times 10^{-5} m/s$ were evaluated in the 10×1 m control volume. The two lowest flow velocities show the same convection pattern as no groundwater flow ([Figure 3](#)). For the reference case and a flow velocity of $3 \times 10^{-5} m/s$ the convection pattern changed to become wavy. Here it was also shown that it would take 110 d to establish the steady-state convection pattern ([Figure 5](#)).

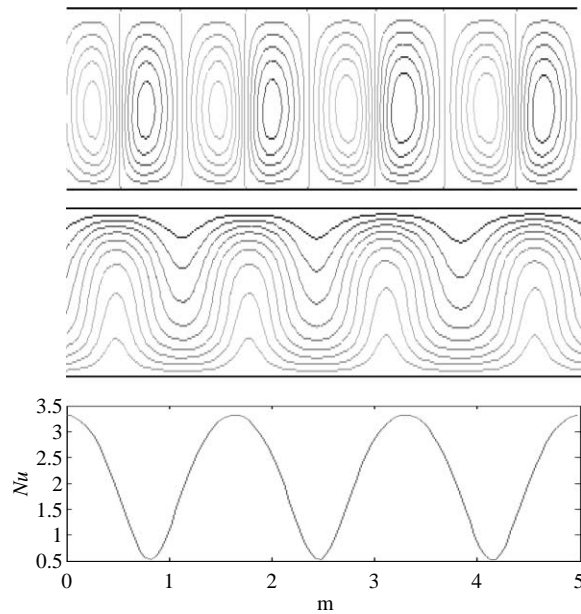


Figure 3 Numerical steady-state solution for part of a 10×1 m control volume shows four pairs of symmetrical convection rolls. $V_i = 3 \times 10^{-8}$ m/s, $Ra = 19$, $K = 6.7 \times 10^{-10}$ m², $T_H = 10^\circ\text{C}$, $T_C = 4^\circ\text{C}$, $Nu = 2.14$. Upper graph: streamlines; middle graph: isotherms; lower graph: Nusselt number

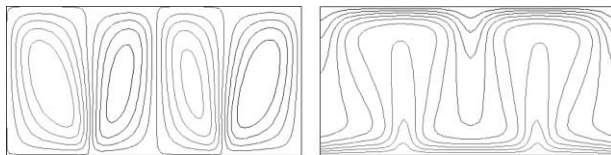


Figure 4 Numerical steady-state solution for a 10×5 m control volume show four symmetrical convection rolls acting in pairs. $V_i = 3 \times 10^{-8}$ m/s, $Ra = 95$, $K = 6.7 \times 10^{-10}$ m², $T_H = 10^\circ\text{C}$, $T_C = 4^\circ\text{C}$, $Nu = 1.17$. Left graph: streamlines; right graph: isotherms

Discussion

An initial horizontal water velocity $V_i = 3 \times 10^{-8}$ m/s was used as a standard disturbance in the simulations. This disturbance triggers the start of convection but does not influence the flow velocities. There are several natural events that would cause similar disturbances, e.g. fluctuating groundwater table because of rain infiltration, air pressure variation and soil heterogeneities.

Monthly mean air temperature records for the south of Sweden (Lund) show that the ambient air temperature is colder than the groundwater temperature during 7 months of the year (METEONORM 2000). The mean air temperature is colder than 4°C during

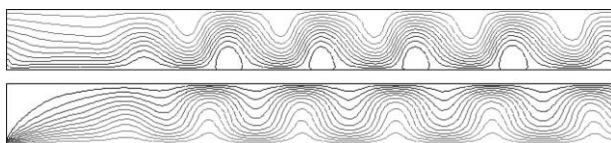


Figure 5 Numerical steady-state solution when horizontal groundwater flow (10^{-6} m/s) is added from left to right in the 10×1 m control volume. $Ra = 19$, $K = 6.7 \times 10^{-10}$ m², $T_H = 10^\circ\text{C}$, $T_C = 4^\circ\text{C}$, $Nu = 2.27$. Upper graph: streamlines; lower graph: isotherms. This pattern should be compared with [Figure 3](#) where no groundwater flow is assumed

approximately 150 d of that time. This means that groundwater at shallow depths will be cooled off during most of the year.

The vertical velocity of the water in the ground is of the order of 3×10^{-5} m/s, when a stable convection pattern is achieved. This means that the water would penetrate to a depth of 1 m within 12 d. Concurrently the water at 1 m depth flows upwards to close the convection roll.

Based on made assumptions the smallest possible permeability for convection to occur is $K = 6.7 \times 10^{-10}$ m², which corresponds to a grain size of 1 mm. This corresponds to a sandy soil while agricultural soil normally consists of finer grains. However, permeability values of soils are mean values, i.e. there are more or less permeable sections in the soil. Natural infiltration of rain and melt water would in such areas rather increase the occurrence of convection.

Since the permeability of an aquifer is a macroscopic mean value, it must include more or less permeable parts. Since any flow follows the path of minimum resistance, groundwater will find its way through the more permeable parts of the soil. This is, however, not considered in performed simulations.

A non-fluctuating horizontal groundwater was assumed in this study. However, laboratory studies on inclined saturated porous media flow models indicate that thermal convection is initiated by such flow (Combarrous and Bories 1975).

Most of the precipitation in southern Sweden (~57% in Lund) falls during the six coldest months of the year. Since snow covers the ground surface only occasionally cold water infiltrates into the ground during most of the winter season. This cools the uppermost groundwater and thereby enhances the thermal convection.

Conclusions

Our hypothesis, that seasonal temperature variation initiates and drives thermal convection, was partly supported by performed simulations for assumed standard conditions.

The number of convection rolls increases with permeability and decreases with the depth of the control volume. Convection rolls form at $Ra > 19$, providing an initial disturbance, a horizontal very small groundwater velocity.

In some cases no stable solution was found although $Nu > 1$, which indicates that part of the heat transport must be a result of convective heat transfer. One explanation could be oscillating or propagating convection rolls, which would not be seen in a steady-state solution.

Small horizontal groundwater velocities ($< 3 \times 10^{-7}$ m/s) through the control volume do not influence the convection though larger flows change the shape of the convection rolls, to become wavy.

Since it takes 110 d to establish steady-state groundwater convection, for assumed standard conditions it is likely to occur in the south of Sweden. Even if the convection was not fully developed vertical groundwater movements will occur.

The critical soil permeability of 6.7×10^{-9} m² for the onset of convection was greater than typical values in agricultural soils. The calculated critical soil permeability corresponds to sandy soil. However, since convection still exists it must also have other explanations. Thus, the simulation model must be developed to include infiltration of rain and melt water, varying groundwater table, inhomogeneous soil permeability and thermal conductivity.

Though transport of nutrients was not included in this model the thermally driven groundwater pattern indicates that it is likely to occur for dissolved nutrients.

Acknowledgements

This study is part of MSc. Maria Engström's PhD work. LTU is gratefully acknowledged for financial support of the project.

References

- Blake, K.R., Bejan, A. and Poulikakos, D. (1984). Natural convection near 4°C in a water saturated porous layer heated from below. *Int. J. Heat Mass Transfer*, **27**, 2355–2364.
- Claesson, J., Efring, B., Eskilson, P. and Hellström, G. (1985a). *Handbook on Thermal Analyses. Part I General*, Report T16-18:1985. Swedish Council for Building Research. Stockholm, Sweden (in Swedish).
- Claesson, J., Efring, B., Eskilson, P. and Hellström, G. (1985b). *Handbook on Thermal Analyses. Part II Heat Storage*, Report T16-18:1985. Swedish Council for Building Research. Stockholm, Sweden (in Swedish).
- Combarous, M.A. and Bories, S.A. (1975). Hydrothermal convection in saturated porous media. *Advances in Hydrosience*, vol 10. Academic Press, New York, pp. 231–307.
- Ene, H.I. and Polisevski, D. (1987). *Thermal Flow in Porous Media*, D. Riedel, Dordrecht.
- Fysikalia-tabell och formelsamling i fysik*, 7th edn. (1991). University Printing Office, Luleå (in Swedish).
- Goren, S. (1966). On free convection in water at 4°C. *Chem. Engng. Sci.*, **21**, 515–518.
- Kundu, P. (1990). *Fluid Mechanics*, Academic Press, New York, p. 355.
- Kyllmar, K. and Johnsson, H. (1998). *Växnäringsförluster till vatten i Typområden på jordbruksmark (JRK) 1984–1995*. SLU, Uppsala, Inst. f. markvetenskap, avd. f. vattenvårdslära, Nr: 44 (in Swedish). Available at: <http://sll.bibul.slu.se/html/sll/slu/ekohydrologi/EHY44/EHY44.HTM>.
- Moore, D.R. and Weiss, N.O. (1973). Nonlinear penetrative convection. *J. Fluid Mech.*, **61**(3), 553–581.
- METEONORM (2000). Meteonorm Version 4.00. Meteotest, Bern, Switzerland. See also: <http://www.meteotest.ch>.
- Nield, D.A. and Bejan, A. (1999). *Convection in Porous Media*, Springer-Verlag, New York.
- Pestov, I. (2000). Numerical techniques for simulating groundwater flow in the presence of temperature gradients. *J. Aust. Math. Soc. Ser. B*, Special issue **42**(E), 1114–1136.
- Rehbinder, G., Gustafsson, G. and Thunvik, R. (1995). *Grundvattenströmningens teori*, KTH, Stockholm, pp. 89–93 (in Swedish).
- Sveriges Nationalatlas (Klimat, sjöar och vattendrag)* (1995). Sveriges nationalatlas (SNA), Stockholm; Höganäs, Bra böcker.
- Versteeg, H.K. and Malalasekera, W. (1995). *An Introduction to Computational Fluid Dynamics, The Finite Volume Method*, Longman Scientific & Technical, Harlow.